RESEARCH ARTICLE

Oxidized low-density lipoprotein promotes vascular endothelial cell dysfunction by stimulating miR-496 expression and inhibiting the Hippo pathway effector YAP

Jun Hu[1,2], Te Liu[3], Zhuang Zhang[4], Yawei Xu[1,5]* and Fu Zhu[2]*

1 Cardiovascular Medicine, Nanjing Medical University, Nanjing 211166, China
2 Xuhui Central Hospital, Shanghai Clinical Research Center, China Academy of Sciences, Shanghai 200031, China
3 Department of Pathology, Yale University School of Medicine, Connecticut 06520, USA
4 Medical School, JiangSu University, Zhengjiang 212013, China
5 Shanghai Tenth People's Hospital, Tongji University, Shanghai 200072, China

Abstract

Oxidized low-density lipoprotein (ox-LDL) can damage vascular endothelial cells and cause atherosclerosis, but its epigenetic regulatory mechanism has not been fully elucidated. We show that ox-LDL induced significant apoptosis and loss of function in human umbilical vascular endothelial cells (HUVECs). At the same time, ox-LDL significantly decreased the expression of Hippo–YAP/ZAP (Yes-associated protein/YLP motif–containing 1) pathway proteins as compared to that of the control. The luciferase reporter system confirmed that microRNA (miR)-496 silenced *YAP* gene expression by binding to its 3′ untranslated region (3′ UTR). Ox-LDL–treated miR-496 overexpression HUVECs had a higher apoptosis rate and more severe dysfunction compared to the control cells. This in-depth study shows that ox-LDL inhibits YAP protein expression by inducing miR-496 expression, leading to its inability to enter the nucleus, thereby losing its function as a transcriptional cofactor for activating the downstream genes. Our findings reveal that, through epigenetic modification, ox-LDL can inhibit the normal expression of Hippo–YAP/ZAP pathway proteins via miR-496 expression and induce vascular endothelial cell dysfunction.

Keywords: Hippo–YAP/ZAP pathway; miR-496; oxidized low-density lipoprotein; vascular endothelial cell

Introduction

Atherosclerosis is an ageing-related vascular disease whose occurrence and development are closely related to the vascular inflammatory response. During atherosclerosis progression, macrophages participate in the local inflammatory responses by secreting cytokines, free radicals, proteases, and various supplements, and mediate low-density lipoprotein (LDL) oxidation by producing reactive oxygen species and reactive nitrogen species, and forming oxidized LDL (ox-LDL) (Bories and Leitinger, 2017; Wong et al., 2017; Xiao et al., 2017). Macrophage phagocytosis of ox-LDL ultimately leads to the formation of macrophage-derived foam cells (Bories and Leitinger, 2017; Wong et al., 2017; Xiao et al., 2017). Sustained high concentrations of ox-LDL can stimulate vascular endothelial cells, upregulate the expression of the autophagy-related proteins beclin 1 and lipidated microtubule-associated protein light chain 3, increase intracellular Ca^{2+} concentration, induce endoplasmic reticulum stress (ERS), and induce the expression of the pro-apoptosis

proteins JNK (mitogen-activated protein kinase 8) and CHOP (DNA damage inducible transcript 3), leading to vascular endothelial cell apoptosis (Muller et al., 2011). In addition, ox-LDL upregulates CHOP through ERS and PERK (eukaryotic translation initiation factor 2 alpha kinase 3) during macrophage-derived foam cell formation to induce macrophage apoptosis and promote the formation of advanced atherosclerosis plaque, fibrous cap, and necrotic center, further enhancing the inflammatory response to promote vascular endothelial cell apoptosis (Seimon et al., 2010). Therefore, ox-LDL plays an important role in atherosclerosis progression. MicroRNAs (miRNAs) comprise a class of 20–23-nucleotide (nt) long non-coding RNA (ncRNA), families that are highly conserved and widely present in eukaryotes. miRNAs have no open reading frame and do not encode a protein product with a specific function, but as single-stranded ncRNAs, they can reverse-complement with the mRNA transcripts of other genes to silence the target genes after transcription. Accumulating studies have demonstrated that miRNAs are involved in various physiological and biochemical reactions in mammals, such as stem cell pluripotency maintenance and directional differentiation regulation, organogenesis, developmental regulation, tumorigenesis and tumor progression, and the pathogenesis of ageing (Cheng et al., 2012; Liu et al., 2013; Moran et al., 2017; Rajman and Schratt, 2017). The Hippo–YAP/TAZ (Yes-associated protein/YLP motif–containing 1) pathway is a kinase cascade consisting of a series of protein kinases and transcription factors. The Hippo signaling pathway is highly conserved from lower to higher animals (Zhao et al., 2011; Zhou, 2014; Cabochette et al., 2015). The pathway primarily consists of three parts: the upstream regulatory elements (NF2 [neurofibromin 2], mer), the core components (MST1/2 [macrophage-stimulating 1 and 2], LATS1/2 [large tumor suppressor kinase 1 and 2]), and the downstream effector molecules (YAP). In normal cells, activated MST1/2 phosphorylates and activates its substrate LATS1/2, which subsequently phosphorylates the downstream effector YAP. Phosphorylated YAP (p-YAP) can bind to 14-3-3 (tyrosine 3-monooxygenase/tryptophan 5-monooxygenase activation protein theta, YWHAQ) in the cytoplasm, where it is sequestered from entering the nucleus, thereby losing its function as a transcriptional cofactor (Zhao et al., 2011; Zhou, 2014; Hindley et al., 2016); YAP is a transcriptional coactivator downstream of the Hippo–YAP/TAZ pathway (Lian et al., 2010; Xie et al., 2012; Cabochette et al., 2015). Under normal conditions, YAP activation promotes cell proliferation and tissue growth. Upon excessive cell or tissue growth, LATS1/2 kinase phosphorylates YAP to prevent it from entering the nucleus, where it acts as a transcriptional cofactor. The loss of nuclear YAP blocks Hippo–YAP/TAZ pathway activity and inhibits further cell and tissue growth (Xie et al., 2012; Cabochette et al., 2015). In addition, YAP

plays an important role in cell division and differentiation, stem cell fate decisions, and tumorigenesis and progression (Zhao et al., 2011; Xie et al., 2012; He et al., 2017; Li et al., 2017; Xiao et al., 2017; Zhang et al., 2017; Zhao et al., 2017; Zhuo and Kang, 2017). Recently, an increasing number of studies have shown that Hippo–YAP/TAZ signaling has emerged as a new pathway for blood vessel development (Park and Kwon, 2018). Azad et al. (2018) reported that the Hippo–YAP pathway is a critical mediator of vascular endothelial growth factor (VEGF)-induced angiogenesis and tumor vasculogenic mimicry. The authors also found that VEGF receptor (VEGFR) activation by VEGF triggers PI3K/MAPK (phosphatidylinositol-4,5-bisphosphate 3-kinase catalytic subunit alpha/mitogen-activated protein kinase) signaling, which subsequently inhibits LATS and activates the Hippo effectors YAP and TAZ. Choi et al. (2015) indicated that overexpression of activated YAP in endothelial cells enhances angiogenic sprouting, which is blocked by angiopoietin-2 depletion or soluble TEK receptor tyrosine kinase treatment. These findings implicate YAP as a critical regulator in angiogenesis and provide new insights into the mechanism coordinating endothelial cell junctional stability and angiogenic activation. In addition, Sakabe et al. (2017) uncovered a previously unrecognized role of cytoplasmic YAP/TAZ in promoting cell migration by activating CDC42 (cell division cycle 42), and described a novel mechanism of Hippo signaling in vascular endothelial cell regulation of angiogenesis. These findings all indicate the central role of YAP, the major transcriptional coactivator of the Hippo pathway, in modulating vascular endothelial cell proliferation, and the strength of endothelial activation and vascular inflammation.

In the present study, we found that ox-LDL upregulates miR-496 expression in human umbilical vein endothelial cells (HUVECs), and suggest that it inhibits Hippo–YAP/ZAP pathway activation by specifically inhibiting YAP expression, ultimately leading to HUVECs apoptosis.

Materials and methods

Isolation of HUVECs

HUVECs were isolated as previously described (Liu et al., 2013), and grown on 1% gelatin-coated culture plates in endothelial basal medium (EBM-2, Lonza) at 37°C in a humidified atmosphere of air containing 5% CO_2.

Animal grouping and drug intervention

A total of six specific pathogen–free (SPF)-grade apolipoprotein E–deficient ($ApoE^{-/-}$) C57/BALB mice and six SPF-grade wild-type (WT) C57/BALB mice were purchased from the Shanghai Research Center for Model Organisms [license number: SCXK (Shanghai) 2015–0018, Shanghai, China]. The

mice were 6–8 weeks old and weighed 30 ± 5 g. After 1 week of adaptive feeding with an ordinary diet, all mice received a high-fat diet daily. The intervention period lasted 6 weeks.

Hematoxylin and eosin (H&E) staining

Mouse aorta was fixed in 10% formaldehyde, and the aortic arch was excised approximately 0.5 cm away from the aortic root. Subsequently, the aorta was routinely dehydrated, embedded in paraffin, serially sectioned at 5-μm thickness (starting from the aortic root), and stained with H&E. The pathological morphology of the aortic tissues was examined under light microscopy.

Masson's trichrome staining

Aortic root sections with atherosclerotic plaques were dewaxed, washed with double-distilled water for 5 min, and incubated with hematoxylin solution for 5–10 min. Following nuclear staining with hematoxylin, the sections were washed thoroughly and stained with Masson's ponceau–acid fuchsin solution for 6–10 min. Subsequently, the sections were washed with 2% glacial acetic acid solution for 5 s, differentiated in 1% phosphomolybdic acid solution for 3–5 min, and stained by direct immersion in aniline blue solution for 5 min. The sections were then washed with 0.2% glacial acetic acid solution for a few seconds, cleared, sealed, and imaged.

Annexin V–FITC/PI (fluorescein isothiocyanate/propidium iodide) staining and flow cytometry

Experiments were performed according to the protocol of an annexin V–FITC apoptosis detection kit (Beyotime Biotechnology, China). Briefly, adherent cells were treated with trypsin to form single-cell suspensions. After washing with phosphate-buffered saline (PBS) and removing the residual fluid by centrifugation, 195 μL annexin V–FITC binding solution was added to gently resuspend the cells. Then, 5 μL annexin V–FITC was added and mixed gently, followed by 10 μL PI staining solution. After incubation in the dark at 20°C for 30 min, detection was performed using a flow cytometer (Cytomics FC 500, Beckman Coulter).

RNA extraction and quantitative real-time PCR (qPCR)

Total RNA was extracted from each group of cells using TRIzol (Invitrogen). After the total RNA was treated with DNase I (Sigma–Aldrich) and quantified, complementary DNA (cDNA) was synthesized using a ReverTra Ace-α First Strand cDNA Synthesis Kit (TOYOBO). qRT-PCR was performed using a RealPlex4 real-time PCR detection system (Eppendorf Co. Ltd., Hamburg, Germany) and SYBR Green Real-Time PCR Master MIX (TOYOBO). The qRT-PCR involved 40 amplification

cycles: denaturation for 15 s at 95°C, annealing for 30 s at 58°C, and extension for 42 s at 72°C. Relative gene expression levels were determined by the comparative threshold cycle ($2^{-\Delta\Delta Ct}$) method, where $\Delta Ct = Ct\_genes - Ct\_18sRNA$, and $\Delta\Delta Ct = \Delta Ct\_all\_groups - \Delta Ct\_blankcontrol\_group$. mRNA expression levels were normalized to 18S rRNA expression levels. Table 1 shows the primer sequences used.

Western blotting

Briefly, total protein was subjected to 12% denaturing sodium dodecyl sulfate–polyacrylamide gel electrophoresis and transferred onto polyvinylidene fluoride membranes (Millipore). After blocking and washing, the membranes were incubated with primary antibodies at 37°C for 45 min [Hippo Signaling Antibody Sampler Kit (Cat No. 8579, Cell Signaling Technology, Inc.)]. After sufficient washing, the membranes were incubated with secondary antibodies at 37°C for 45 min, and then washed in TBST at room temperature for 4×14 min. Finally, the membranes were developed using enhanced chemiluminescence (Pierce Biotechnology; Sigma–Aldrich Chemical).

miR-496 overexpression oligonucleotide RNA

The miR-496 and miR-496 mutant (miR-mut) oligonucleotide RNAs were purchased from GenePharma (Shanghai, China). HUVECs were co-transfected with Lipofectamine

Table 1 PCR primer sequences.

Gene product	Sequence (5′ →3′)	Size (bp)
YAP1	Forward (F): GTTGGGAGATGGCAAAGACA	109
	Reverse (R): ACGTTCATCTGGGACAGCAT	
TAZ	F: GGCTGGGAGATGACCTTCAC	96
	R: ATTCATCGCCTTCCTAGGGT	
14-3-3ζ	F: AGCAGATGGCTCGAGAATACA	103
	R: GAAGCATTGGGGATCAAGAA	
14-3-3ε	F: ATCTGGTGTACCAGGCGAAG	101
	R: AACTGTCAGCTCCACATCCA	
14-3-3β	F: AAAGTGCATTTTGCCCATTC	104
	R: TGGCTTTCTGTACCAGCTCA	
14-3-3η	F: GGAGCGCTACGACGACAT	101
	R: TCTTGTAGGCCACAGAGAGGA	
14-3-3θ	F: AGAAAGTGGAGTCCGAGCTG	131
	R: CCGGAAGTAATCACCCTTCA	
MST1	F: TCCTGCTGCTTCTGACTCAA	96
	R: GCAGGTGCTGTAGCTCTGTG	
MSt2	F: AGGCTATAACTGTGTGGCCG	128
	R: GTGGTGGATTTGTGGGAATC	
LATS1	F: TTTCTTGGCACAAACACCAT	130
	R: GGGTCCTCGGCAAAGTTTA	
18S rRNA	F: CGTTGATTAAGTCCCTGCCCTT	202
	R: TCAAGTTCGACCGTCTTCTCAG	

3000 according to the manufacturer's protocol to transfer 0.2 μg miR-496 or miR-mut oligonucleotide RNA.

Luciferase reporter assay

The luciferase reporter assay was performed as described elsewhere (Cheng et al., 2012; Mitamura et al., 2014). Briefly, 1.5×10^4 mouse NIH-3T3 cells were seeded in white 96-well plates on Day 1 and transfected with reporter constructs on Day 2 using Lipofectamine 3000. The luciferase activity was measured using assay reagent 48 h after transfection. The WT or mutant *Yap1* 3′ untranslated region (3′UTR) sequence was inserted downstream of the firefly luciferase reporter gene, which was controlled by the SV40 enhancer for expression in mammalian cells, whereas no oligonucleotides were inserted in the control vector (GeneCopoeia, Rockville, MD, USA). *Renilla* luciferase was used as a tracking indicator for successful transfection. The luciferase activity was measured using LightSwitch Assay Reagent (SwitchGear Genomics) according to the manufacturer's instructions.

Capillary tubule formation assay

All steps were performed according to a previous report (Liu et al., 2013). Briefly, HUVECs were seeded on Matrigel-coated 6-chamber slides (2.0×10^5 cells/chamber) in the presence and absence of the test substances described in the cell migration assay section. After 12-h incubation in a CO_2 incubator, the cells were photographed. To calculate the data, the number of branch points in four non-overlapping fields was determined.

Wound-healing assay

All steps of the assay were conducted according to a previously described protocol (Zhang et al., 2011). Each group of cells were grown to confluence, and then scratched using a 200-μL pipette tip. Three wounds were made for each sample, and all were photographed at the zero time point and at subsequent time points. The assays were repeated thrice for each clone.

Statistical analysis

Each experiment was performed at least three times; data shown are the means ± SE, where applicable; differences were evaluated using the Student *t*-test. $P < 0.05$ was considered to indicate statistically significant differences.

Results

High-fat diet induced aortic root lesions and Hippo–YAP/ZAP pathway downregulation in ApoE$^{-/-}$ mice

A large number of atherosclerotic plaques developed at the aortic root in the ApoE$^{-/-}$ mice. Moreover, some of the plaques were on the verge of rupture. The lesions in the ApoE$^{-/-}$ mice had advanced into the atherosclerotic plaque stage. Compared with the WT mice, ApoE$^{-/-}$ mice exhibited a significantly increased area of plaques (Figure 1). Masson's trichrome staining revealed that, compared with the WT mice, ApoE$^{-/-}$ mice had significantly increased lipid infiltration area in aortic root plaques (Figure 1). Furthermore, immunofluorescence staining indicated significantly decreased expression of Hippo–YAP/ZAP pathway components (LATS1, MOB1 [MOB kinase activator 1A], YAP1, p-YAP1) in the ApoE$^{-/-}$ mice, but not in the WT mice (Figure 1). These results suggest that a high-fat diet can induce aortic root lesions and Hippo–YAP/ZAP pathway downregulation in ApoE$^{-/-}$ mice.

Ox-LDL induced miR-496 expression but decreased Hippo–YAP/ZAP pathway expression

At 24 h after ox-LDL treatment, mRNA expression levels of the key Hippo–YAP/ZAP pathway genes (*Mst1*, *Lats1*, *Yap1*, *Ywhab* [14-3-3β]) were significantly lower than that of the control group (Figures 2 and S1). Bioinformatics analysis (http://www.microrna.org/microrna/home.do) showed that the mature miR-496 and *Yap* mRNA 3′UTR (346 nt–352 nt) had seven consecutive matching nucleotides (Figure 2). Ox-LDL increased miR-496 expression significantly (Figure 2). WT miR-496 overexpression in NIH-3T3 cells significantly inhibited the activity of luciferase carrying the *Yap* 3′UTR sequence. In contrast, miR-mut was unable to silence the expression of luciferase carrying the *Yap* 3′UTR sequence (Figure 2). HUVECs with exogenous miR-496 overexpression had significantly reduced endogenous YAP expression (Figure 2). These results demonstrate that ox-LDL specifically downregulates Hippo–YAP/ZAP pathway member expression and upregulates miR-496 expression. miR-496 may silence YAP expression by directly binding to its 3′UTR.

miR-496 overexpression induced HUVEC apoptosis and dysfunction

To verify that miR-496 has a regulatory effect on vascular endothelial cell function, we overexpressed miR-496 in HUVECs. After 72 h, fluorescence-activated cell sorting (FACS) revealed that cells overexpressing miR-496 had significantly higher apoptosis rates than the control (miR-mut–transfected) cells (Figure 3). The in vitro angiogenesis experiments demonstrated that miR-496 overexpression decreased lumen formation in Matrigel as compared to control cells (Figure 3). Scratch assays suggested that miR-496 also decreased cell migration rates (Figure 3). Furthermore, Transwell chamber experiments revealed that significantly fewer cells migrated through the filter when miR-496 was overexpressed (Figure 3). Together, these results suggest
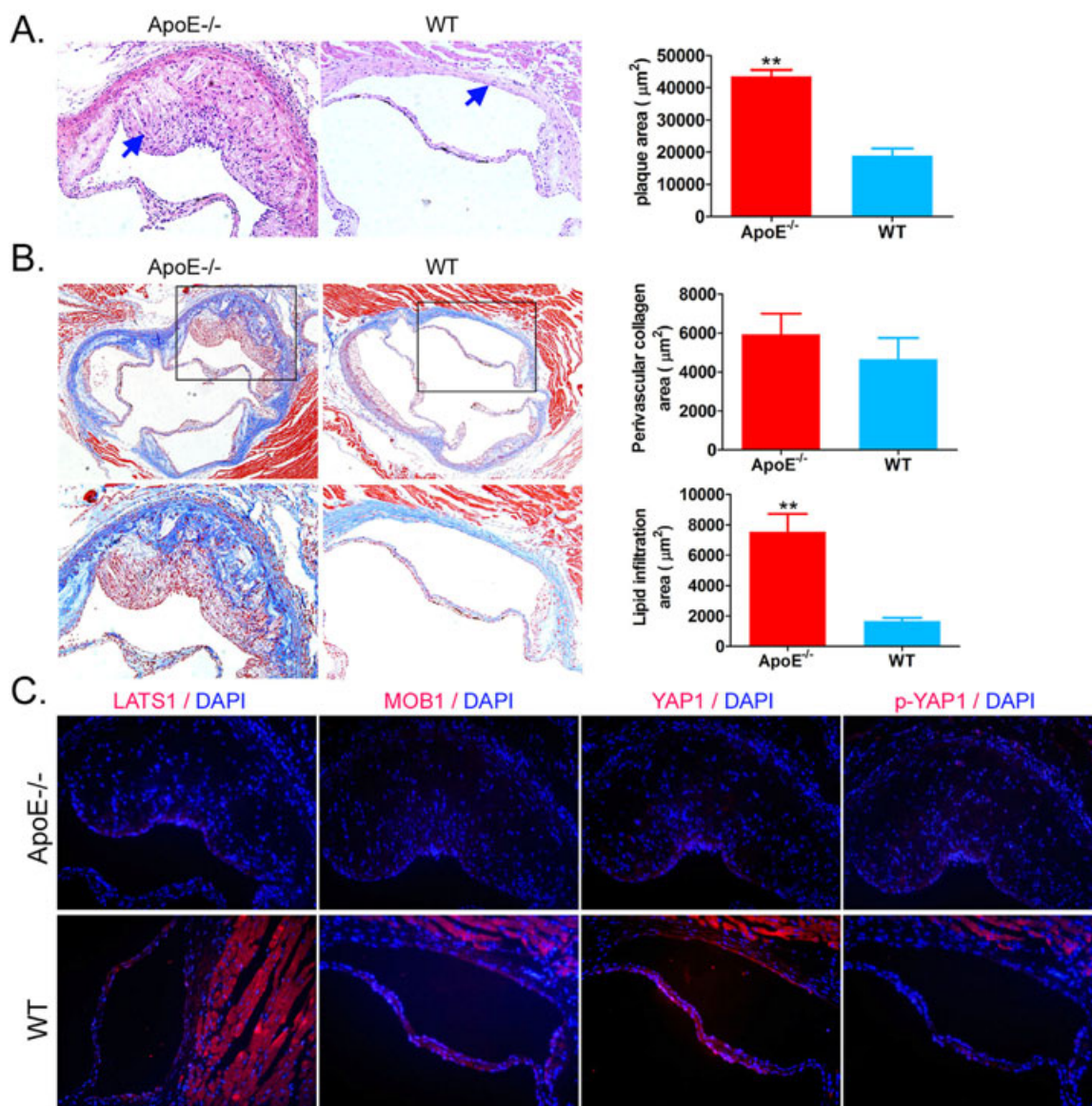
Figure 1 High-fat diet–induced aortic root lesions and Hippo–YAP/ZAP pathway downregulation in ApoE$^{-/-}$ mice. (A) A large number of atherosclerotic plaques at the aortic root in ApoE$^{-/-}$ mice. Arrow indicates a plaque. Magnification: 200×; H&E staining. **$P < 0.01$ versus ApoE$^{-/-}$ mice; n = 6. (B) Compared with WT mice, ApoE$^{-/-}$ mice have significantly increased lipid infiltration area in aortic root plaques. Magnification: 100×, inset magnification: 200×; Masson's trichrome staining. **$P < 0.01$ versus ApoE$^{-/-}$ mice; n = 6. (C) Significantly decreased expression of Hippo-YAP/ZAP pathway components in ApoE$^{-/-}$ mice. Magnification: 200×; immunofluorescence staining.

that exogenous miR-496 induces significant HUVEC apoptosis and dysfunction.

Exogenous miR-496 overexpression exacerbated ox-LDL–induced HUVEC apoptosis and dysfunction

We transfected HUVECs with miR-496 or miR-mut (control) in the presence or absence of ox-LDL. After 72 h, ox-LDL–miR-496 cells had a significantly higher total apoptosis rate than the control cells (Figures 4 and S1). In

vitro angiogenesis assays revealed that ox-LDL–miR-496 cells had significantly lower lumen forming ability in Matrigel than the control cells (Figure 4). The scratch assays showed that ox-LDL–miR-496 cells migrated significantly smaller distances than the control cells (Figure 4). Transwell chamber experiments also showed significantly fewer migrated ox-LDL–miR-496 cells than control cells (Figure 4). These results suggest that exogenous miR-496 overexpression exacerbates ox-LDL–induced HUVEC apoptosis and dysfunction.
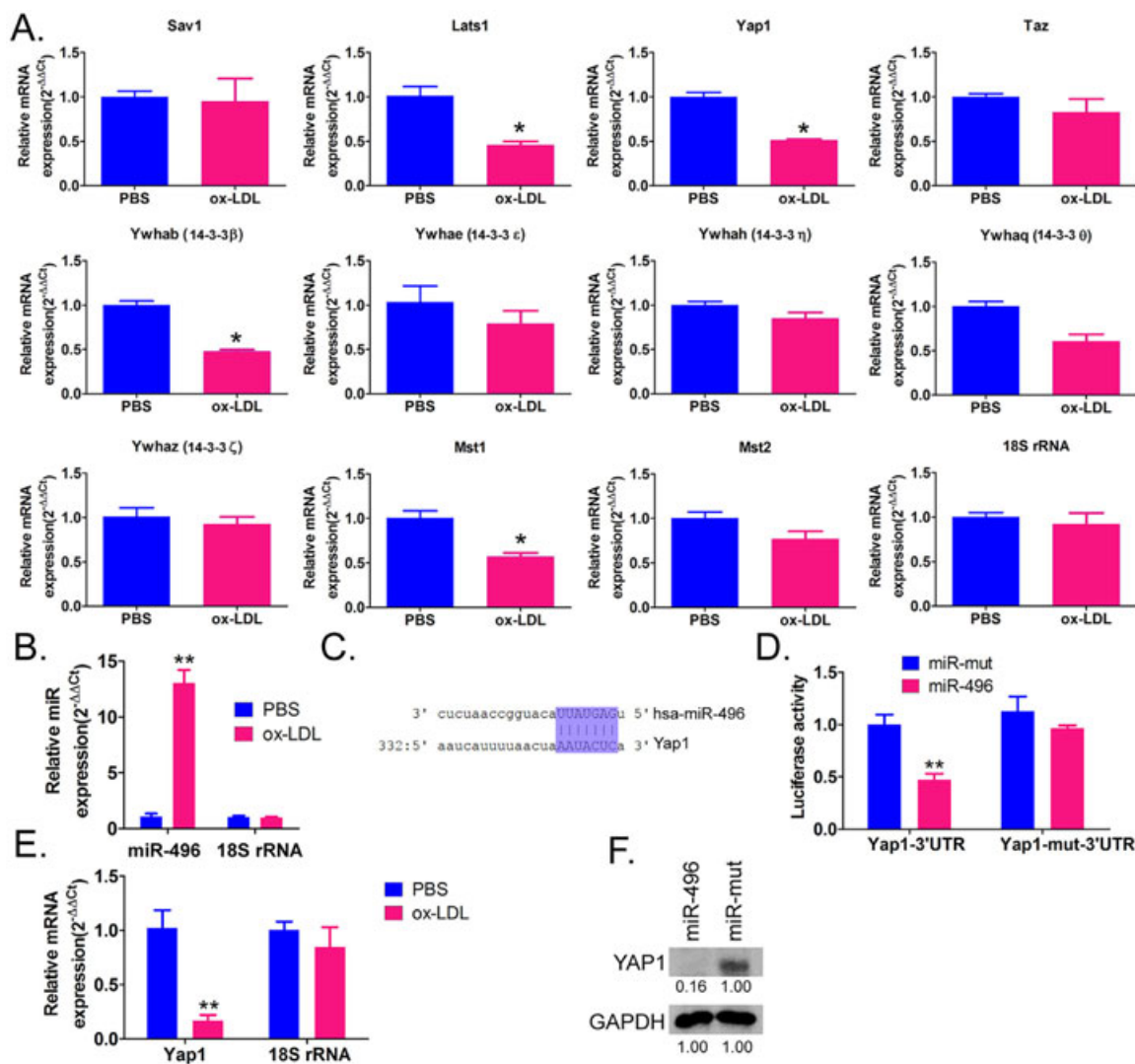
Figure 2 **Ox-LDL upregulated miR-496 and downregulated the Hippo–YAP/ZAP pathway.** (A) Ox-LDL–treated HUVECs had significantly lower mRNA levels of *MST1*, *LATS1*, *YAP1*, and *YWHAB* (14-3-3β) 24 h after treatment as compared to the control group; *$P < 0.05$ versus PBS; n = 3. (B) The ox-LDL-treated group had significantly higher miR-496 expression as compared to the control group; **$P < 0.01$ versus PBS; n = 3. (C) Bioinformatics analysis showing that mature miR-496 and the *Yap1* mRNA 3′UTR (346 nt–352 nt) had seven consecutive matching nucleotides. (D) Luciferase reporter assays suggesting that WT miR-496 overexpression in NIH-3T3 cells significantly inhibited the activity of luciferase carrying the *Yap1* 3′UTR sequence. miR-mut could not silence the expression of luciferase carrying the *Yap1* 3′UTR sequence. **$P < 0.01$ versus PBS; n = 3. (E) Exogenous miR-496 overexpression significantly reduced endogenous *Yap1* mRNA expression levels; **$P < 0.01$ versus PBS; n = 3. (F) Exogenous miR-496 overexpression significantly reduced endogenous YAP1 protein expression. **$P < 0.01$ versus PBS; n = 3.

Exogenous miR-496 overexpression significantly downregulated Hippo–YAP/ZAP expression

Cells overexpressing miR-496 had significantly lower levels of nuclear YAP1 protein than control cells or untransfected cells (Figure 4). Cells overexpressing miR-496 had significantly lower MST1/2, MOB1, SAV1 (salvador family WW domain–containing protein 1), p-MOB1, and vascular endothelial marker VEGFR2 expression levels than the control cells (Figure 5), but had significantly higher activated caspase-3 protein expression than the control cells (Figure 5).

However, 14-3-3β protein expression was not significantly changed (Figure 5). Therefore, miR-496 overexpression significantly inhibits the expression of endogenous Hippo–YAP/ZAP pathway proteins in HUVECs.

Discussion

In recent years, an increasing number of studies have confirmed that the Hippo–YAP/ZAP pathway plays an important role in vascular remodeling and related
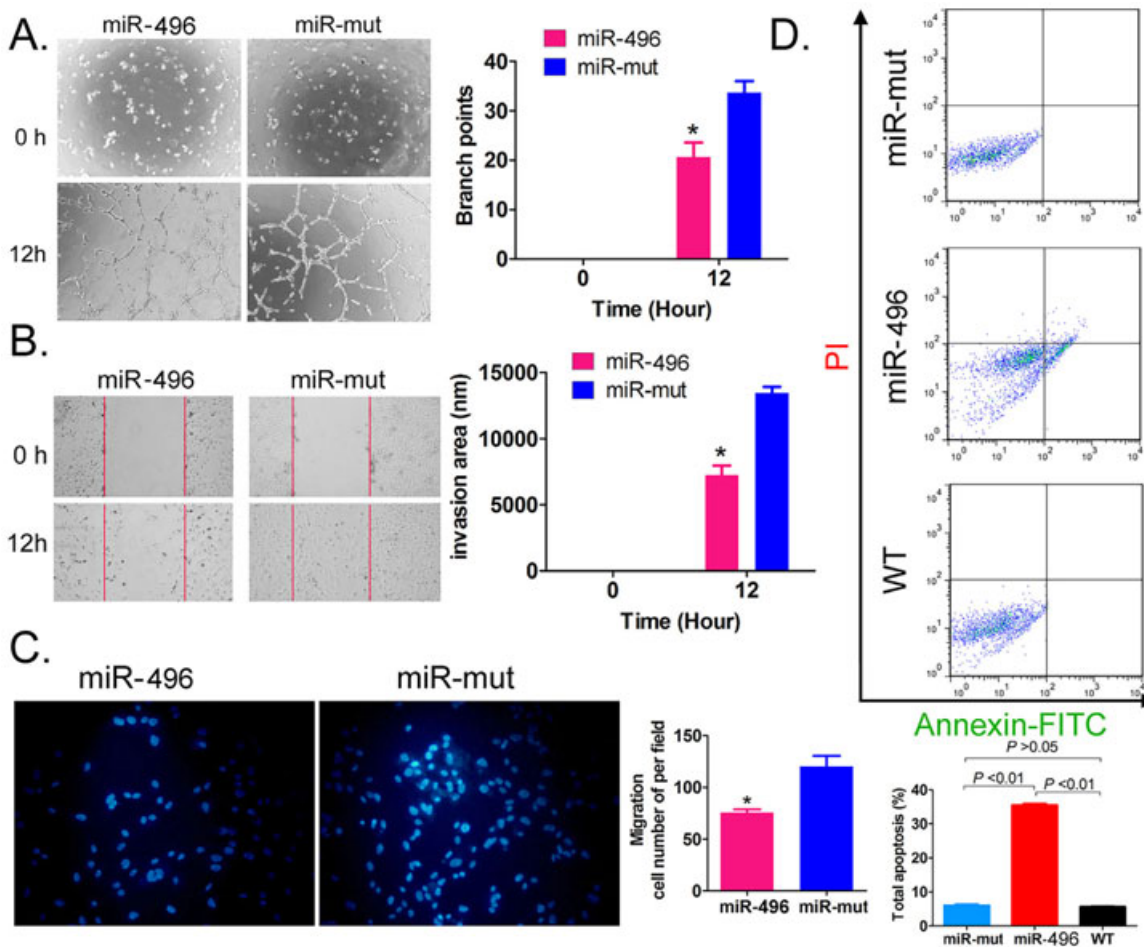
Figure 3 miR-496 overexpression induced HUVEC apoptosis and dysfunction. (A) miR-496 overexpression HUVECs had significantly lower lumen forming ability in Matrigel than control cells; $*P < 0.05$ versus miR-mut; n = 3. (B) Significantly decreased migration rates of miR-496 overexpression HUVECs to the center of the scratch compared to control cells; $*P < 0.05$ versus miR-mut; n = 3. (C) Significantly fewer migrated miR-496 overexpression HUVECs compared to control cells; $*P < 0.05$ versus miR-mut; n = 3. (D) Significantly higher total apoptosis rate of miR-496 overexpression HUVECs compared to control cells.

cardiovascular diseases. The Hippo–YAP/ZAP pathway can alter extracellular matrix production and degradation, and vascular endothelial and smooth muscle cell growth, apoptosis, and migration, thereby allowing vascular remodeling during cardiovascular disease progression, such as pulmonary hypertension, atherosclerosis, restenosis after angioplasty, and aortic aneurysm (He et al., 2017). In addition, specific *Yap1* knockout in mouse cardiomyocytes blocked myocardial cell proliferation, causing myocardial dysplasia and ultimately leading to premature embryonic death. Normal *Yap* expression in mice may promote increased embryonic heart volume and myocardial cell development, promoting myocardial regeneration and contraction after myocardial infarction by inducing myocardial cell proliferation (Zhou, 2014). Nakajima et al. found that *yap1* mutation in zebrafish led to the loss of vascular stability. Furthermore, they found that adjusting the blood

flow to induce nuclear YAP1 translocation in vascular endothelial cells could regulate the expression of filamentous actin and angiomotin, thereby inducing the expression of auxiliary transcription factors (Nakajima et al., 2017). Xie et al. (2012) reported that rapid YAP1 upregulation after injury to the vascular smooth muscle stimulated PDGF-BB (platelet-derived growth factor BB) expression effectively, a factor that induces phenotypic switching of vascular smooth muscle cells. When *YAP1* was knocked out in cultured vascular smooth muscle cells, cell proliferation was attenuated due to increased serum response factor binding to the CArG region of specific contraction control genes. In addition, in the study of atherosclerosis using ApoE$^{-/-}$ mice, Xiao et al. (2017) found that the interaction between TFPI-1 (tissue factor pathway inhibitor) and angiomotin resulted in decreased YAP phosphorylation and a further increase in the expression of genes involved in vascular
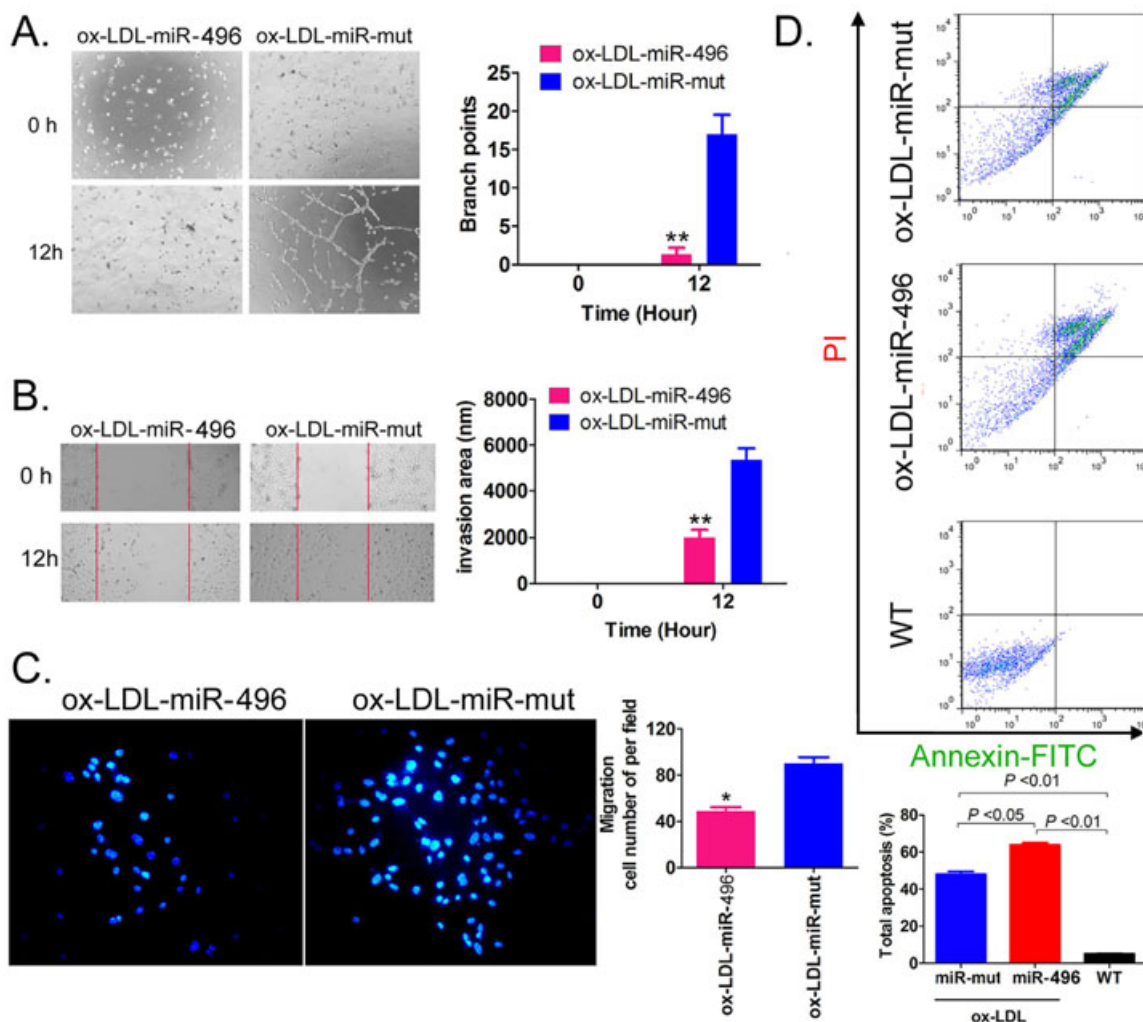
Figure 4 Exogenous miR-496 overexpression exacerbated ox-LDL–induced HUVEC apoptosis and dysfunction. (A) ox-LDL–miR-496 overexpression HUVECs had significantly lower ability to form a lumen in Matrigel compared to control cells; $^{**}P < 0.01$ versus control (ox-LDL–miR-mut); n = 3. (B) Significantly smaller migration area to the center of the scratch in the ox-LDL–miR-496 group than in the control group; $^{**}P < 0.01$ versus control (ox-LDL–miR-mut); n = 3. (C) Significantly fewer migrated ox-LDL–miR-496 overexpression HUVECs compared to control cells; $^{**}P < 0.01$ versus control (ox-LDL–miR-mut); n = 3. (D) Significantly higher total apoptosis rate in ox-LDL–miR-496 overexpression HUVECs compared to the control cells.

smooth muscle cell proliferation and migration, thereby accelerating the occurrence of atherosclerosis. Therefore, the Hippo–YAP/ZAP pathway plays an important regulatory role in the normal physiological activity and pathogenesis of the cardiovascular system.

Previous studies have reported that microRNAs specifically target key factors in the Hippo–Yap/ZAP pathway, such as LATS1, TAZ, MST1/2, and YAP1 (Peng et al., 2009; Lin et al., 2013; Chaulk et al., 2014; Mitamura et al., 2014; Tian et al., 2015). However, the majority of these studies focused on tumor cell proliferation, invasion, and epithelial–mesenchymal transformation (Thompson and Cohen, 2006; Seton-Rogers, 2014). Here, we focused on the effect of ox-LDL on Hippo–Yap/TAZ pathway member expression in

vascular endothelial cells. Ox-LDL treatment significantly downregulated the endogenous expression of key factors in the Hippo–Yap/TAZ pathway, including LATS1, YAP1, and MST1, which are critical pathway components. The lack of expression of the above factors significantly alters the pathway's biological effects. We hypothesized that ox-LDL induced changes in the expression of several microRNAs and that this change may directly affect Hippo–Yap/TAZ pathway member expression level. Based on this hypothesis, we explored the microRNAs targeting the *Yap1* gene. We found that miR-496 has consecutive specific complementarity sites with the 3′UTR of *Yap1* mRNA. Through molecular biology experiments, we demonstrated that miR-496 overexpression silenced endogenous *YAP1* expression effectively
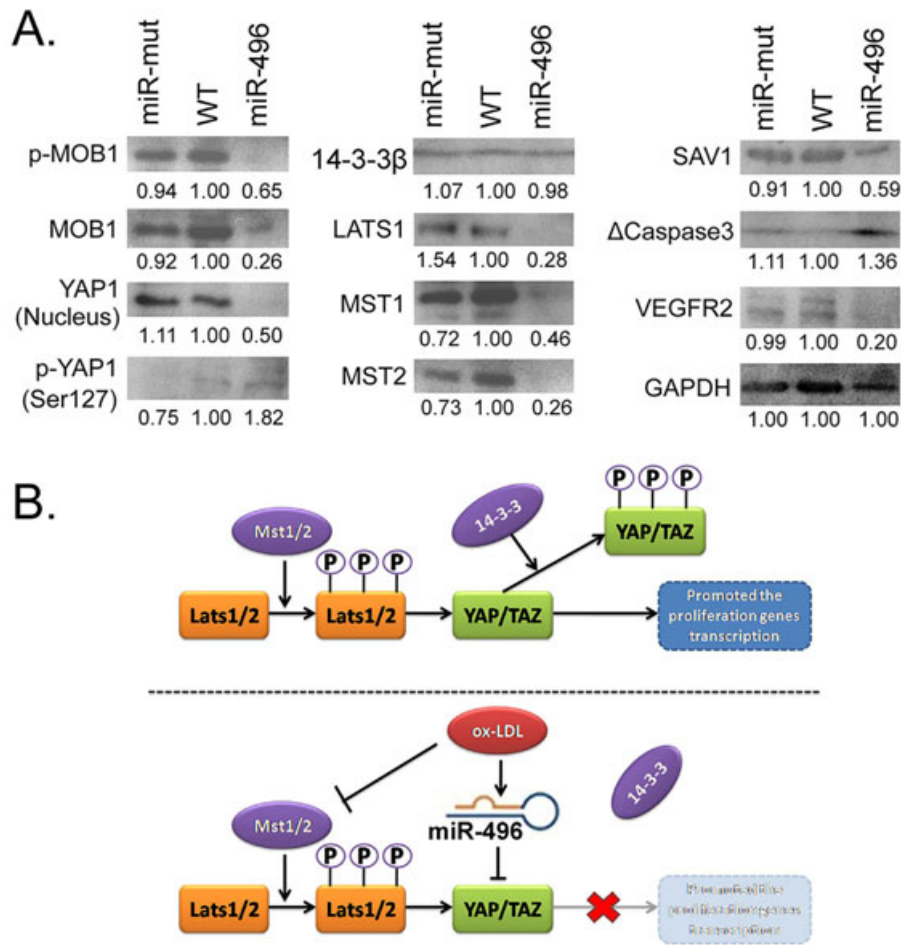
Figure 5 Exogenous miR-496 overexpression significantly downregulated Hippo–YAP/ZAP pathway expression. (A) miR-496 overexpression decreased YAP1, MST1/2, MOB1, SAV1, p-MOB1, and VEGFR2 protein expression levels. (B) The ox-LDL–miR-496–Hippo–YAP/ZAP pathway relationship.

in vascular endothelial cells. At the same time, endogenous miR-496 expression protected cells against ox-LDL. The results suggest that ox-LDL affects endogenous miR-496 expression. Ox-LDL stimulation combined with miR-496 overexpression affected vascular endothelial cell proliferation and migration more severely, a much stronger effect than either condition alone. Therefore, our study clarifies that ox-LDL specifically silences *YAP1* gene expression by upregulating endogenous miR-496 expression in vascular endothelial cells, thereby inhibiting Hippo–Yap/TAZ pathway expression and weakening vascular endothelial cell proliferation and migration (Figure 5).

Conclusions

We identify a novel mechanism of epigenetic modification of the Hippo–Yap/TAZ pathway, which is inactivated by ox-LDL stimulation.

References

Azad T, Janse van Rensburg HJ, Lightbody ED, Neveu B, Champagne A, Ghaffari A, Kay VR, Hao Y, Shen H, Yeung B, Croy BA, Guan KL, Pouliot F, Zhang J, Nicol CJB, Yang X (2018) A LATS biosensor screen identifies VEGFR as a regulator of the Hippo pathway in angiogenesis. Nat Commun 9: 1061.

Bories GFP, Leitinger N (2017) Macrophage metabolism in atherosclerosis. FEBS Lett 591: 3042–60.

Cabochette P, Vega-Lopez G, Bitard J, Parain K, Chemouny R, Masson C, Borday C, Hedderich M, Henningfeld KA, Locker M, Bronchain O, Perron M (2015) YAP controls retinal stem

cell DNA replication timing and genomic stability. eLife 4: e08488.

Chaulk SG, Lattanzi VJ, Hiemer SE, Fahlman RP, Varelas X (2014) The Hippo pathway effectors TAZ/YAP regulate dicer expression and microRNA biogenesis through Let-7. J Biol Chem 289: 1886–91.

Cheng W, Liu T, Wan X, Gao Y, Wang H (2012) MicroRNA-199a targets CD44 to suppress the tumorigenicity and multidrug resistance of ovarian cancer-initiating cells. FEBS J 279: 2047–59.

Choi HJ, Zhang H, Park H, Choi KS, Lee HW, Agrawal V, Kim YM, Kwon YG (2015) Yes-associated protein regulates endothelial cell contact-mediated expression of angiopoietin-2. Nat Commun 6: 6943.

He J, Bao Q, Yan M, Liang J, Zhu Y, Wang C, Ai D (2018) The role of Hippo/yes-associated protein signalling in vascular remodelling associated with cardiovascular disease. Br J Pharmacol 175(8): 1354–61.

Hindley CJ, Condurat AL, Menon V, Thomas R, Azmitia LM, Davis JA, Pruszak J (2016) The Hippo pathway member YAP enhances human neural crest cell fate and migration. Sci Rep 6: 23208.

Li C, Wang S, Xing Z, Lin A, Liang K, Song J, Hu Q, Yao J, Chen Z, Park PK, Hawke DH, Zhou J, Zhou Y, Zhang S, Liang H, Hung MC, Gallick GE, Han L, Lin C, Yang L (2017) A ROR1-HER3-lncRNA signalling axis modulates the Hippo-YAP pathway to regulate bone metastasis. Nat Cell Biol 19: 106–19.

Lian I, Kim J, Okazawa H, Zhao J, Zhao B, Yu J, Chinnaiyan A, Israel MA, Goldstein LS, Abujarour R, Ding S, Guan KL (2010) The role of YAP transcription coactivator in regulating stem cell self-renewal and differentiation. Genes Dev 24: 1106–18.

Lin CW, Chang YL, Chang YC, Lin JC, Chen CC, Pan SH, Wu CT, Chen HY, Yang SC, Hong TM, Yang PC (2013) MicroRNA-135b promotes lung cancer metastasis by regulating multiple targets in the Hippo pathway and LZTS1. Nat Commun 4: 1877.

Liu T, Shen D, Xing S, Chen J, Yu Z, Wang J, Wu B, Chi H, Zhao H, Liang Z, Chen C (2013) Attenuation of exogenous angiotensin II stress-induced damage and apoptosis in human vascular endothelial cells via microRNA-155 expression. Int J Mol Med 31: 188–96.

Mitamura T, Watari H, Wang L, Kanno H, Kitagawa M, Hassan MK, Kimura T, Tanino M, Nishihara H, Tanaka S, Sakuragi N (2014) MicroRNA 31 functions as an endometrial cancer oncogene by suppressing Hippo tumor suppressor pathway. Mol Cancer 13: 97.

Moran Y, Agron M, Praher D, Technau U (2017) The evolutionary origin of plant and animal microRNAs. Nat Ecol Evol 1(3): 27.

Muller C, Salvayre R, Negre-Salvayre A, Vindis C (2011) HDLs inhibit endoplasmic reticulum stress and autophagic response induced by oxidized LDLs. Cell Death Differ 18: 817–28.

Nakajima H, Yamamoto K, Agarwala S, Terai K, Fukui H, Fukuhara S, Ando K, Miyazaki T, Yokota Y, Schmelzer E, Belting HG, Affolter M, Lecaudey V, Mochizuki N (2017) Flow-Dependent Endothelial YAP Regulation Contributes to Vessel Maintenance. Dev Cell 40: 523–36 e6.

Park JA, Kwon YG (2018) Hippo-YAP/TAZ signaling in angiogenesis. BMB Rep 51: 157–62.

Peng HW, Slattery M, Mann RS (2009) Transcription factor choice in the Hippo signaling pathway: homothorax and yorkie regulation of the microRNA bantam in the progenitor domain of the Drosophila eye imaginal disc. Genes Dev 23: 2307–19.

Rajman M, Schratt G (2017) MicroRNAs in neural development: from master regulators to fine-tuners. Development 144: 2310–22.

Sakabe M, Fan J, Odaka Y, Liu N, Hassan A, Duan X, Stump P, Byerly L, Donaldson M, Hao J, Fruttiger M, Lu QR, Zheng Y, Lang RA, Xin M (2017) YAP/TAZ-CDC42 signaling regulates vascular tip cell migration. Proc Natl Acad Sci USA 114: 10918–23.

Seimon TA, Nadolski MJ, Liao X, Magallon J, Nguyen M, Feric NT, Koschinsky ML, Harkewicz R, Witztum JL, Tsimikas S, Golenbock D, Moore KJ, Tabas I (2010) Atherogenic lipids and lipoproteins trigger CD36-TLR2-dependent apoptosis in macrophages undergoing endoplasmic reticulum stress. Cell Metab 12: 467–82.

Seton-Rogers S (2014) Tumour suppressors: Hippo promotes microRNA processing. Nat Rev Cancer 14: 216–7.

Thompson BJ, Cohen SM (2006) The Hippo pathway regulates the bantam microRNA to control cell proliferation and apoptosis in Drosophila. Cell 126: 767–74.

Tian Y, Liu Y, Wang T, Zhou N, Kong J, Chen L, Snitow M, Morley M, Li D, Petrenko N, Zhou S, Lu M, Gao E, Koch WJ, Stewart KM, Morrisey EE (2015) A microRNA-Hippo pathway that promotes cardiomyocyte proliferation and cardiac regeneration in mice. Sci Transl Med 7: 279ra38.

Wong BW, Marsch E, Treps L, Baes M, Carmeliet P (2017) Endothelial cell metabolism in health and disease: impact of hypoxia. EMBO J 36: 2187–203.

Xiao J, Jin K, Wang J, Ma J, Zhang J, Jiang N, Wang H, Luo X, Fei J, Wang Z, Yang X, Ma D (2017) Conditional knockout of TFPI-1 in VSMCs of mice accelerates atherosclerosis by enhancing AMOT/YAP pathway. Int J Cardiol 228: 605–14.

Xie C, Guo Y, Zhu T, Zhang J, Ma PX, Chen YE (2012) Yap1 protein regulates vascular smooth muscle cell phenotypic switch by interaction with myocardin. J Biol Chem 287: 14598–605.

Zhang L, Liu T, Huang Y (2011) Liu J. microRNA-182 inhibits the proliferation and invasion of human lung adenocarcinoma cells through its effect on human cortical actin-associated protein. Int J Mol Med 28: 381–8.

Zhang S, Chen Q, Liu Q, Li Y, Sun X, Hong L, Ji S, Liu C, Geng J, Zhang W, Lu Z, Yin ZY, Zeng Y, Lin KH, Wu Q, Li Q, Nakayama K, Nakayama KI, Deng X, Johnson RL, Zhu L, Gao D, Chen L, Zhou D (2017) Hippo signaling suppresses cell ploidy and tumorigenesis through skp2. Cancer Cell 31: 669–84 e7.

Zhao B, Tumaneng K, Guan KL (2011) The Hippo pathway in organ size control, tissue regeneration and stem cell self-renewal. Nat Cell Biol 13: 877–83.

Zhao Y, Fei X, Guo J, Zou G, Pan W, Zhang J, Huang Y, Liu T, Cheng W (2017) Induction of reprogramming of human amniotic epithelial cells into iPS cells by overexpression of Yap,

Oct4, and Sox2 through the activation of the Hippo-Yap pathway. Exp Ther Med 14: 199–206.

Zhou J (2014) An emerging role for Hippo-YAP signaling in cardiovascular development. J Biomed Res 28: 251–4.

Zhuo W, Kang Y (2017) Lnc-ing ROR1-HER3 and Hippo signalling in metastasis. Nat Cell Biol 19: 81–3.

Supporting Information

Additional supporting information may be found online in the Supporting Information section at the end of the article.

Figure S1. The transcription regulation of YAP on downstream gene.